Percolative vortex motion in high-temperature superconductors

Michael Ziese*

Vrije Universiteit Amsterdam, Faculty of Physics and Astronomy, De Boelelaan 1081, 1081 HV Amsterdam, The Netherlands

A model for percolative vortex motion in inhomogeneous superconductors is introduced. Near the percolation threshold the linear, frequency-dependent electronic conductivity is found to obey scaling laws. The percolation model for vortex motion provides an alternative explanation to the experimental finding of scaling in the electronic conductivity that is conventionally attributed to a vortex glass transition. The critical exponents derived from simulations of bond percolation on three-dimensional lattices are in satisfying agreement with critical exponents obtained from the scaling analysis of the conductivity of $YBa_2Cu_3O_{7-\delta}$ twinned single crystals and ceramics. The electronic conductivity is calculated in an effective medium approximation and is compared to experimental data.

I. INTRODUCTION

In high-temperature superconductors large thermal fluctuations due to the high operating temperatures and small pinning energies lead to considerable vortex motion even at small driving currents. The vortex motion in the linear regime is most favorably investigated by measurements of the frequency-dependent electronic conductivity $\sigma(\omega)$. According to theoretical considerations,[1,2] in samples with strong random pinning disorder three regions of a qualitatively different vortex response are expected in the vortex glass phase, the vortex liquid phase, and near the vortex glass transition temperature T_g. At low temperatures the vortex system is in a glassy phase and a weak frequency dependence of the vortex response to ac currents is found.[3,4] Near the transition between the glassy and the liquid vortex phases the electronic conductivity obeys scaling laws[1,2] and far above the transition the motion of the vortex liquid is diffusive.[5–7]

The existence of a scaling regime for the linear, frequency-dependent conductivity[8–10] $\sigma(\omega)$ and the nonlinear dc conductivity[11,12] $\sigma(j)$ is firmly established. Though these experimental findings in transport quantities support the existence of a vortex glass transition, measurements of thermodynamic variables have not shown an indication of a phase transition. Moreover, recent theoretical investigations even show the absence of a vortex glass transition in more realistic models of three-dimensional (3D) superconductors with a finite screening length.[13] Thus the evidence for the existence of a vortex glass transition is still doubtful.

In this work an alternative explanation to the vortex glass theory, i.e., a model of percolative vortex motion in inhomogeneous superconductors is proposed. The model of percolative vortex motion accounts for the existence of a critical scaling regime in transport quantities. In this model the percolation transition corresponds to the vortex glass transition derived from scaling analyses. The limiting forms of the scaling functions are identical to the predictions of vortex glass theory.

Besides the vortex glass theory a variety of phenomenological models has been developed for the thermally activated flux motion. The thermally activated hopping of vortex bundles out of their pinning potentials results in a linear current-voltage characteristic at low currents.[14] Using the linear current voltage characteristic Kes *et al.*[5] and Geshkenbein *et al.*[15] developed a simple theory for the ac response of a superconducting sample that is described as a normal conductor with a frequency-independent resistivity of thermally activated form (TAFF). This theory was extended by Coffey and Clem[6] and Brandt[7] to include pinning effects, flux flow, and losses due to the normal fluid component.

The extended TAFF theory was successfully used to describe surface impedance measurements in the GHz region.[16] A semiquantitative agreement was found for ac susceptibility measurements on $Bi_2Sr_2CaCu_2O_8$ single crystals[17] and for vibrating reed measurements on $YBa_2Cu_3O_{7-\delta}$ single crystals and films.[18] Reed *et al.*[8] and Kötzler *et al.*[9,10] showed that the extended TAFF model was in quantitative agreement with the frequency-dependent ac susceptibility of Y-1:2:3 single crystals and films near T_c, whereas the ac susceptibility at lower temperatures was in agreement with the existence of critical fluctuations around a vortex glass transition temperature T_g.

In this work simple expressions for the electronic conductivity are derived in an effective medium approximation (EMA). The EMA provides the frequency-dependent conductivity far from the percolation transition. Furthermore, the EMA predictions are a first approximation for the crossover region from the scaling regime near the percolation threshold to the mean field regime far from threshold.

II. CALCULATION OF THE ELECTRONIC CONDUCTIVITY IN A PERCOLATION MODEL

A. General model

Different pinning mechanisms are usually present in high-temperature superconductors. Especially at high temperatures pinning by twin planes has proved to be strong for magnetic fields tilted by an angle $<10°–20°$ with respect to the c axis of the superconductor.[19] It is expected that pinning by different extended defects, e.g., grain boundaries and inclusions, is equally well important. The intrinsic pinning of vortices by the layered crystal structure seems to be relevant only at rather small angles $<2°$ between the CuO_2 planes and the magnetic field.[20] In single crystals as well as in thin

films a further pinning mechanism, i.e., pinning of vortices by point defects, is important. Resistive measurements of the range of the pinning potential in Y-1:2:3 thin films yielded very small values $\sim 5-10$ Å consistent with core pinning of vortices by point defects.[21] Therefore inhomogeneities even on a small length scale can lead to deviations from a homogeneous vortex flow. Since the material processing of the high-temperature superconducting oxides is quite complex, inhomogeneous distributions of material defects can be expected. Interlaced regions of different pinning potential strength that consist of regions of different point defect density or of regions with extended pinning centers form a percolation network for vortex motion.[22,23]

In the following the vortex motion in an inhomogeneous superconductor will be described in a bond percolation model on a lattice. Consider randomly distributed regions with different pinning strengths. At high temperatures vortices in the weak pinning regions are unpinned, whereas vortices in strong pinning regions are already pinned. Since the local pinning potential is a function of temperature T and magnetic field B, the extensions of these regions change upon variation of temperature and field. Let p denote the concentration of regions with an unpinned flux line lattice with $p \to 0$ for $T \to 0$ and $p \to 1$ for $T \to T_c$. For convenience the pinned and unpinned vortex lattices will be called vortex glass and vortex liquid, respectively. In this context vortex glass means a pinned, disordered vortex lattice. The frequency-dependent vortex diffusivities in the zero current limit are denoted by $D_{VG}(T,B,\omega)$ and $D_{VL}(T,B,\omega)$ in the glass and liquid phases, respectively.

The macroscopic vortex diffusivity $D(T,B,\omega)$ is obtained after averaging the local diffusivities over the sample volume. The averaging procedure will be performed in a bond percolation model which represents the superconductor by a regular lattice. A bond of this lattice lying with probability p in the vortex liquid phase is assigned a diffusivity D_{VL}, whereas it has a diffusivity D_{VG}, if it is with probability $q = 1 - p$, in the vortex glass phase. The averaged vortex diffusivity is[24]

$$D = D_{VL}F(p,h), \tag{1}$$

where F denotes an unkown function and $h = D_{VG}/D_{VL}$ the diffusivity ratio.

Under the application of a current $\vec{j}$ the vortices start to move and generate an electric field $\vec{E} = \rho(T,\vec{b},\omega)\vec{j}$. ρ denotes the averaged electronic resistivity and $\vec{b}$ the local magnetic field averaged over a few vortex spacings. With the induction law $\nabla \times \vec{E} = -\partial \vec{b}/\partial t$ and Ampère's law $\nabla \times \vec{b} = \mu_0 \vec{j}$ a nonlinear diffusion equation

$$\nabla \times (\rho \nabla \times \vec{b}) = -\mu_0 \frac{\partial \vec{b}}{\partial t} \tag{2}$$

is obtained. In the following the experimental situation is considered in which a small frequency-dependent magnetic field $\delta \vec{B} \propto \exp(i\omega t)$ is superimposed on a large dc field $\vec{B}$, i.e., $\vec{b} = \vec{B} + \delta \vec{B}$. Linearization of Eq. (2) leads to a linear diffusion equation for the disturbance[25] $\delta \vec{B}$,

$$\frac{\rho}{\mu_0} \nabla^2 \delta \vec{B} = \frac{\partial \delta \vec{B}}{\partial t}, \tag{3}$$

with the averaged vortex diffusivity $D = \rho/\mu_0$. Therefore the electronic conductivity $\sigma = \rho^{-1}$ is related to the vortex diffusivity by

$$\sigma = [\mu_0 D]^{-1} = [\mu_0 D_{VL}F(p,h)]^{-1}. \tag{4}$$

Equation (4) is valid if normal fluid losses can be neglected.

The function $F(p,h)$ can be determined numerically or in an effective medium approximation that will be discussed in Sec. II D. In Sec. II C scaling laws near the percolation threshold are investigated. In the next section expressions for the vortex diffusivities D_{VG} and D_{VL} in the pinned and unpinned vortex regions are derived.

B. Estimation of vortex diffusivities

The vortex diffusivities in the vortex glass and vortex liquid phases are derived from the averaged equation of vortex motion,[26]

$$\eta \vec{v} + \beta \vec{v} \times \hat{B} = \vec{j} \times \vec{B} + \vec{F}_p, \tag{5}$$

where $\vec{v}$ denotes the vortex velocity, $\vec{F}_p$ the pinning force, and $\hat{B}$ a unit vector along the direction of the magnetic field. η is the vortex viscosity and β the coefficient of the Magnus force. If $\vec{F}_p$ is known, Eq. (5) can be solved for $\vec{v}$ and the diffusivity is then obtained from $\vec{E} = \vec{B} \times \vec{v}$ and Maxwell's equations.

1. Unpinned flux line lattice

In the vortex liquid phase the pinning force F_p leads to a renormalization of the viscous term but not of the Magnus force term in Eq. (5). The moving flux line lattice experiences an additional friction due to the interaction with the pinning sites,[26] i.e., $\vec{F}_p = -\eta^* \vec{v}$ with an effective vortex viscosity $\eta^* \propto \exp(U/k_B T)$. U is a typical activation barrier for vortex hopping. Introducing $\tilde{\eta} = \eta + \eta^*$ one obtains the vortex velocity $\vec{v}$ from Eq. (5),

$$\vec{v} = \frac{B}{\tilde{\eta}^2 + \beta^2}(\tilde{\eta}\vec{j} \times \hat{B} + \beta \vec{j}), \tag{6}$$

and the electric field

$$\vec{E} = \frac{B^2}{\tilde{\eta}^2 + \beta^2}(\tilde{\eta}\vec{j} + \beta\hat{B} \times \vec{j}). \tag{7}$$

From the linearized diffusion equation (3) one obtains the vortex liquid diffusivity

$$D_{VL} = \frac{\tilde{\eta}B^2}{\mu_0(\tilde{\eta}^2 + \beta^2)}. \tag{8}$$

2. Pinned flux line lattice

In the vortex glass phase the vortices perform small oscillations about their equilibrium sites under the influence of a small driving current $\vec{j} \propto \exp(i\omega t)$. Assuming a harmonic pin-

ning potential at small vortex displacements $\vec{u}$ the pinning force is given by $\vec{F}_p = -\alpha\vec{u}$ with the Labusch parameter[27] α. Since $\vec{u} \propto \exp(i\omega t)$ and $\vec{v} = i\omega\vec{u}$, the vortex glass diffusivity is given by

$$D_{\text{VG}} = \frac{\left(\eta + \dfrac{\alpha}{i\omega}\right)B^2}{\mu_0\left[\left(\eta + \dfrac{\alpha}{i\omega}\right)^2 + \beta^2\right]}. \qquad (9)$$

Brandt[7] proposed to include thermally activated vortex hopping out of the pinning potential by substituting α by the Fourier transform of $\dot{\alpha}$. If an exponential decay of the Labusch parameter is assumed, $\alpha(t) = \alpha\exp(-t/\tau_p)$, α has to be substituted by[7] $\alpha/(1 - i/\omega\tau_p)$. $\tau_p \propto \exp(U/k_BT)$ denotes a "pinning time," i.e., the mean time the vortex is bound to the pinning center.

The inclusion of a Magnus force term in the equation of vortex motion, Eq. (5), leads to a renormalization of the vortex diffusivities. Since the Magnus force term is only important at high frequencies $\omega > \tau_\beta^{-1} = \alpha/\beta$, it will be neglected in the following.

C. Scaling regime

In the critical region around the percolation threshold p_c the averaged electronic conductivity assumes the scaling form[24]

$$\sigma = \frac{1}{\mu_0 D_{\text{VL}}}|\Delta p|^{-t}\Sigma_\pm(h|\Delta p|^{-t-s}), \qquad (10)$$

with $\Delta p = p - p_c$ and $h = D_{\text{VG}}/D_{\text{VL}}$. Following the standard notation[24] the critical exponents are called t and s; an interchange with the time variable that is also called t is unlikely since the time variable is not used in this and the following sections. The scaling functions $\Sigma_+(x)$ in the vortex liquid ($p > p_c$) and $\Sigma_-(x)$ in the vortex glass ($p < p_c$) phase assume the asymptotic forms[24]

$$\Sigma_+(x) \xrightarrow{\quad x \to 0 \quad} \text{const}, \qquad (11)$$

$$\Sigma_-(x) \xrightarrow{\quad x \to 0 \quad} \frac{\text{const}}{x}, \qquad (12)$$

$$\Sigma_\pm(x) \xrightarrow{\quad |x| \to \infty \quad} \text{const} \times x^{-t/(t+s)}. \qquad (13)$$

$x = h|\Delta p|^{-t-s}$ denotes the scaling variable. In the effective medium approximation the scaling functions in d dimensions are

$$\Sigma_\pm(x) = \frac{2(d-1)}{[d^2 + 4(d-1)x]^{1/2} \pm d}, \qquad (14)$$

with $t = s = 1$.

The concentration p of vortex liquid regions cannot be easily accessed experimentally. The percolation threshold p_c is identified with the vortex glass transition temperature

T_g obtained from scaling analyses of the electronic conductivity. Near the transition it is plausible to assume $\Delta p \propto |T - T_g|^\zeta$.

For a further discussion of the scaling functions the conductivity ratio h is expressed by the vortex diffusivities, Eq. (8) and Eq. (9), derived in the previous section. The Magnus force term is neglected, i.e., $\beta = 0$. Since[7] $\eta^* \propto \exp(U/k_BT) \gg \eta$, one obtains $D_{\text{VL}} \simeq B^2/\mu_0\eta^* \propto \exp(-U/k_BT)$. For not too large frequencies $\omega\tau_\eta \ll 1$, with $\tau_\eta = \eta/\alpha$, one obtains from Eq. (9) a purely inductive vortex glass diffusivity $D_{\text{VG}} \simeq i\omega\lambda_c^2$. λ_c denotes the Campbell penetration depth,[28] $\lambda_c = (B^2/\mu_0\alpha)^{1/2}$. In YBa$_2Cu_3O_{7-\delta}$ samples the relaxation time τ_η is estimated to $\tau_\eta \simeq 10^{-10}$ s for single crystals[29] and thin films.[30]

Inserting the diffusivity ratio $h = i\omega/\omega_0$ with $\omega_0 = D_{\text{VL}}/\lambda_c^2$ in Eq. (10) one realizes that the percolation model predicts the same scaling law as the vortex glass theory.[1,2] In the limit $(\omega/\omega_0)|\Delta p|^{-t-s} \ll 1$ one obtains $\sigma \propto |\Delta p|^{-t}$ above the percolation transition and $\sigma \propto |\Delta p|^s/(i\omega)$ below the transition; i.e., the linear dc resistivity $\rho_{\text{dc}} = \lim_{\omega \to 0}\sigma^{-1}(\omega)$ vanishes at the percolation transition and $\rho_{\text{dc}} = 0$ in the vortex glass phase. This result is consistent with the description of the nonlinear dc resistivity $\rho(j)$ in the vortex glass phase. The pinned vortex lattice is described by an effective activation barrier[1] $U(j)$ that diverges for small current densities $j \to 0$ such that $\rho(j) \propto \exp[-U(j)/k_BT] \to 0$ in the linear regime considered here. The full treatment of the nonlinear percolation problem is beyond the scope of this work. There are indications in the literature that the nonlinear dc conductivity $\sigma(j)$ calculated in a percolation model obeys scaling laws similar to the scaling laws of vortex glass theory.[31] Yamafuji and Kiss[32] have recently derived scaling laws for the nonlinear dc resistivity in a model that considers a critical current distribution. These scaling laws are indeed similar to the scaling laws of vortex glass theory.

The phase angle $\Phi = \arctan(\sigma''/\sigma')$ of the electronic conductivity at the percolation transition $\Delta p = p - p_c = 0$ is

$$\Phi(p = p_c) = \frac{\pi}{2}\left(1 - \frac{s}{t+s}\right). \qquad (15)$$

Since the scaling laws of the percolation model and the vortex glass model are equivalent, one obtains the following relationship between the critical exponents of the two models:

$$t\zeta = \nu(z-1), \qquad (16)$$

$$s\zeta = \nu. \qquad (17)$$

The critical exponents ν and z of the vortex glass model are defined by the divergence of the vortex glass correlation length $\xi_{\text{VG}} \propto |T - T_g|^{-\nu}$ and the time scale for critical fluctuations, $\tau_{\text{VG}} \propto \xi_{\text{VG}}^z$.

Since the exponent ζ is not known, only the ratio $t/s = z - 1$ can be compared with theoretical estimates for the critical exponents of percolation theory.

In Table I the critical exponents ν and z derived from measurements of the frequency-dependent conductivity of YBa$_2$Cu$_3$O$_{7-\delta}$ samples are summarized. For twinned

TABLE I. Critical exponents of $YBa_2Cu_3O_{7-\delta}$ samples obtained from the scaling of the linear, frequency-dependent conductivity.

$\vec{B}$	ν	z	Reference
Twinned $YBa_2Cu_3O_{7-\delta}$ single crystals			
$\parallel \hat{c}$	0.69 ± 0.13	3.0 ± 0.4	33
$\parallel \hat{c}$	0.70 ± 0.05	3.0 ± 0.3	8
$\parallel \hat{c}$	3.1 ± 0.3	3.1 ± 0.3	9
$\perp \hat{c}$	1.6 ± 0.3	6.3 ± 0.3	9
$\parallel \hat{c}$	3.1	3.1	34
$YBa_2Cu_3O_{7-\delta}$ films			
$\parallel \hat{c}$	1.1 ± 0.4	5.2 ± 0.6	35
$\parallel \hat{c}$		3.70 ± 0.46	36
$\parallel \hat{c}$	1.7 ± 0.1	5.5 ± 0.5	10
$\parallel \hat{c}$	2.0 ± 0.5	5.5 ± 1.0	37
$\parallel \hat{c}$		3.34 ± 0.64	30
$\parallel \hat{c}$		6.0 ± 2.0	30
$YBa_2Cu_3O_{7-\delta}$ ceramic			
	3.0 ± 0.4	3.0 ± 0.4	38

Y-1:2:3 single crystals in a magnetic field parallel to the c axis, in a ceramic Y-1:2:3 sample and in two Y-1:2:3 films $z \simeq 3.0$ is found. However, the values for the Y-1:2:3 films obtained in Refs. 30 and 36 are only derived from the critical loss angle $\Phi(T_g)$ instead of performing a full scaling analysis. Therefore these values have to be viewed with some care. Olsson *et al.*,[35] Kötzler *et al.*,[10] and Baselgia Stahel *et al.*[37] found values $z > 5$ for Y-1:2:3 films. These values are in agreement with critical exponents obtained from the scaling of the nonlinear dc resistivity.[11]

For the twinned Y-1:2:3 single crystals ($\vec{B} \parallel \hat{c}$) and the Y-1:2:3 ceramic one obtains a mean value for the ratio of the critical exponents,

$$t/s = z - 1 = 2.0 \pm 0.4, \qquad (18)$$

whereas for Y-1:2:3 films ($\vec{B} \parallel \hat{c}$) the ratio

$$t/s = z - 1 = 4.4 \pm 0.7 \qquad (19)$$

seems more appropriate.

In Table II the critical exponents for percolation on a lattice are summarized. The ratio $t/s = 2.60 \pm 0.14$ obtained for lattice percolation in $d = 3$ dimensions is in satisfying agreement with the experimentally determined value $t/s = 2.0 \pm 0.4$ for twinned Y-1:2:3 single crystals and Y-1:2:3 ceramics. However, it is considerably lower than the

TABLE II. Theoretical critical exponents for bond percolation networks.

	t	s	$t/s = z - 1$	Reference
EMA	1.0	1.0	1.0	24
$d = 2$	1.299 ± 0.002	1.299 ± 0.002	1.0	39
$d = 3$	1.9 ± 0.1	0.73 ± 0.01	2.60 ± 0.14	40,41

value found for Y-1:2:3 films. The duality symmetry leads in two dimensions to the value[24] $t/s = 1$, which is not consistent with the experimental data.

Continuum percolation problems (''Swiss cheese'' models) can be mapped on lattice percolation problems with a distribution of bond strengths,[42]

$$g(D_V) \propto D_V^{-a}, \qquad (20)$$

where D_V denotes a local vortex diffusivity. It is found that the critical exponents $\bar{t}$ and $\bar{s}$ in these systems can be considerably enhanced over their counterparts t and s in simple lattice models. If one considers the lower bounds for $\bar{t}$ and $\bar{s}$ given by Feng *et al.*[42] to be exact, as was suggested by Lubensky and Tremblay,[43] one obtains

$$\bar{t} = \lambda(d - 2) + \frac{1}{1 - a}, \qquad (21)$$

$$\bar{s} = \lambda(2 - d) + \frac{1}{1 - a}. \qquad (22)$$

λ denotes the geometric exponent of the percolation correlation length $\xi_p \propto |\Delta p|^{-\lambda}$.

In $d = 3$ dimensions one has $\lambda = 0.875$.[24] Interpreting the ratio $t/s = 4.4 \pm 0.6$ observed for Y-1:2:3 films as arising from a distribution of bond diffusivities one obtains $a = 0.28 \pm 0.05$.

These findings might be interpreted as follows. The satisfying agreement between the experimentally determined and the calculated value of the ratio t/s for Y-1:2:3 twinned crystals and ceramics indicates that two pinning mechanisms with different pinning strengths exist in these materials. The two pinning mechanisms lead to well-defined regions of pinned and unpinned flux lines. Thus a simple lattice percolation model with two bond strengths is appropriate. The two pinning mechanisms might be related to point defect pinning and pinning by twin boundaries, respectively.

The results for the Y-1:2:3 films indicate that in thin films a continuous distribution of pinning strengths is present.

D. Effective medium approximation

Well outside the critical region the averaged diffusivity D is well described within the effective medium approximation (EMA).[44] If D_V denotes a local vortex diffusivity and $f(D_V)$ the distribution function for the vortex diffusivity, the averaged diffusivity D can be obtained from[45,46,44]

$$\int f(D_V) \frac{D - D_V}{D_V + (d - 1)D} dD_V = 0. \qquad (23)$$

d denotes the dimension of the system.

In the following only the binary distribution $f(D_V) = p\,\delta(D_{VL}) + q\,\delta(D_{VG})$ with $q = 1 - p$ will be considered. $\delta(x)$ denotes Dirac's delta function. In this case the electronic conductivity is given by

$$\sigma = \sigma' - i\sigma'' = \frac{1}{\mu_0 D_{VL}} \frac{2(1-p_c)}{(p-p_c)+(q-p_c)h+A^{1/2}}, \quad (24)$$

$$A = (p-p_c)^2 + (q-p_c)^2 h^2 + 2(p_c - p_c^2 + pq)h, \quad (25)$$

with $p_c = d^{-1}$ and $h = D_{VG}/D_{VL}$.

It was shown in the previous section that at low frequencies $\omega \ll \tau_\eta^{-1} = \alpha/\eta \approx 10$ GHz (Refs. 16,30) the vortex glass diffusivity is well approximated by $D_{VG} = i\omega\lambda_c^2$, yielding an imaginary diffusivity ratio

$$h = i\frac{\omega}{\omega_0}. \quad (26)$$

Since the vortex liquid diffusivity D_{VL} and the Labusch parameter α at the transition temperature T_g are not well known, it is difficult to estimate the frequency scale ω_0. From high-frequency surface impedance measurements on Y-1:2:3 films[16] α can be estimated to $\alpha \sim 10^{17}-10^{20}$ N/m^4 at high temperatures and $B = 1$ T. Using typical resistivities of Y-1:2:3 films at the irreversibility line[18] that is close to the glass transition line one obtains $D_{VL} \sim 10^{-5}-10^{-2}$ m^2 s^{-1} and therefore $\omega_0 \sim 10^6-10^{12}$ Hz at $B = 1$ T. In the following calculated values of the conductivity modulus $|\sigma| = (\sigma'^2 + \sigma''^2)^{1/2}$ and the loss tangent

$$\tan(\Phi) = \frac{\sigma''}{\sigma'} \quad (27)$$

are compared to experimental values. Since the experimental values were obtained in the critical region and the EMA is valid well outside the critical region, the comparison between theory and experiment only shows qualitative agreement.

In Figs. 1(a) and 1(b) the loss tangent $\tan(\Phi)$ and the modulus $|\sigma|$ of the electronic conductivity of a 250 nm thin Y-1:2:3 film in a field $B = 0.4$ T are shown as a function of frequency. The data were obtained by Kötzler et al.[10] from the numerical inversion of the frequency-dependent ac susceptibility. The phase angle $\Phi(T_g) = 0.82(\pi/2)$ at the transition temperature $T_g = 88.9$ K is independent of frequency in agreement with the scaling law, Eq. (15).

In Figs. 2 (a) and 2(b) the loss tangent $\tan(\Phi)$ and conductivity modulus $|\sigma|$ according to the extended TAFF model are shown. The curves are calculated with Eq. (9) including the effect of thermally activated vortex hopping by the introduction of an exponentially relaxing Labusch parameter. The conductivity is normalized by the flux flow conductivity $\sigma_{FF} = \eta/B^2$. The curves are calculated in the absence of a Magnus force, $\tau_\beta = \beta/\alpha = 0$, for different values of the viscosity $\tau_\eta = \eta/\alpha$. For large pinning times $\tau_p \gg \tau_\eta$ the loss tangent is large, i.e., $\tan(\Phi) \gg 1$, and a frequency-independent plateau value $\Phi = \pi/2$ is observed at low frequencies $\omega \ll \tau_\eta^{-1}$ in contrast to the experimentally determined nontrivial value $\Phi(T_g) = 0.82(\pi/2)$.
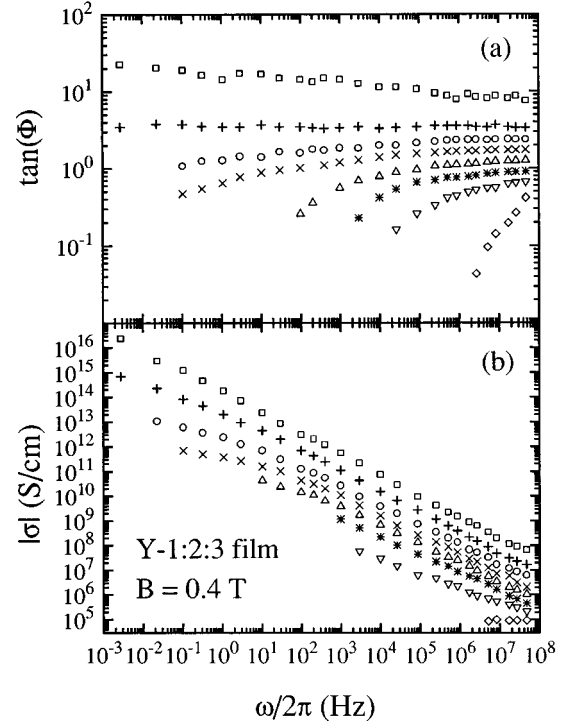

FIG. 1. (a) Loss tangent and (b) modulus of the electronic conductivity of a Y-1:2:3 film as a function of frequency at $B = 0.4$ T. The data are taken from Ref. 10. □, 88.0 K; +, 88.9 K; ○, 89.1 K; △, 89.3 K; ▽, 89.6 K; ◇, 90.0 K.
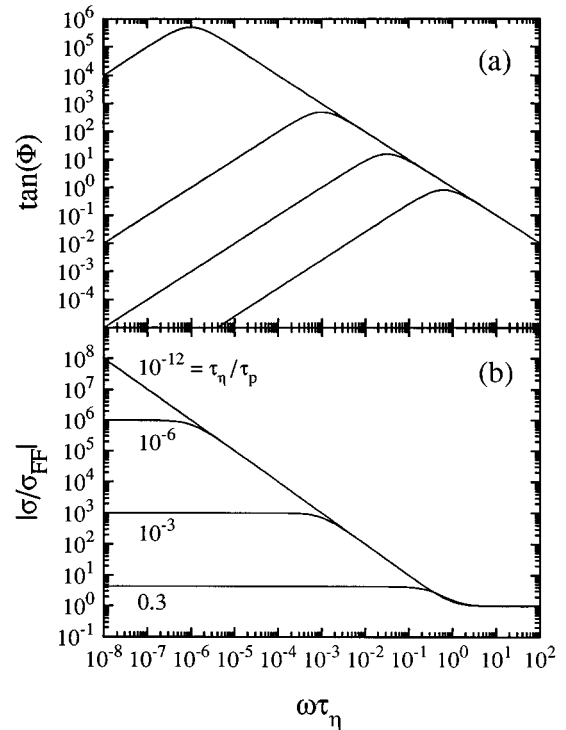

FIG. 2. (a) Loss tangent and (b) modulus of the electronic conductivity in the extended TAFF model; see Eq. (9). The conductivity is normalized to the flux flow conductivity. The curves are calculated with the parameter values $\tau_\eta/\tau_p = 10^{-12}$, 10^{-6}, 10^{-3}, 0.3 and $\tau_\beta = 0$.
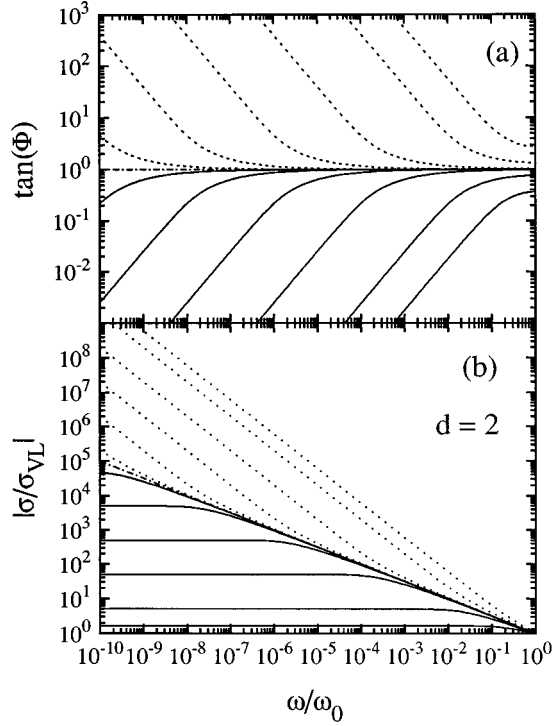
FIG. 3. (a) Loss tangent and (b) modulus of the electronic conductivity in the effective medium approximation for $d=2$ dimensions. The parameters are $\tau_\beta=0$ and $\tau_\eta=0$. The dash-dotted line is the percolation transition $p=p_c$, and the dotted and solid lines are calculated in the vortex glass and vortex liquid phase for concentrations $|\Delta p|=10^{-5}$, 10^{-4}, 10^{-3}, 10^{-2}, 10^{-1}, 0.3.
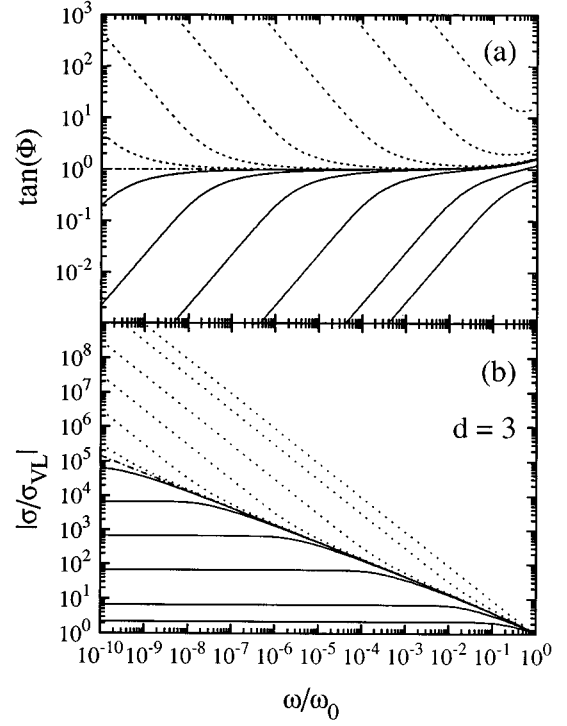
FIG. 4. (a) Loss tangent and (b) modulus of the electronic conductivity in the effective medium approximation for $d=3$ dimensions. The parameters are $\tau_\beta=0$ and $\tau_\eta=0$. The dash-dotted line is the percolation transition $p=p_c$, and the dotted and solid lines are calculated in the vortex glass and vortex liquid phase for concentrations $|\Delta p|=10^{-5}$, 10^{-4}, 10^{-3}, 10^{-2}, 10^{-1}, 0.3.

The loss tangent $\tan(\Phi)$ and conductivity modulus $|\sigma|$ calculated in the effective medium approximation are shown in Figs. 3(a) and 3(b) and 4(a) and 4(b) for $d=2$ and $d=3$, respectively. The conductivity is normalized by the conductivity in the vortex liquid state, $\sigma_{VL}=(\mu_0 D_{VL})^{-1}$. The dash-dotted lines in the figures correspond to the percolation transition $\Delta p=0$, and the dotted and solid lines are calculated in the vortex glass ($\Delta p=-10^{-5}$, -10^{-4}, $\ldots$, -0.1, -0.3) and vortex liquid phase ($\Delta p=10^{-5}$, 10^{-4}, $\ldots$, 0.1, 0.3), respectively. In both dimensions $d=2$ and $d=3$ one finds a critical phase angle $\Phi(p_c)=\pi/4$ at low frequencies in contrast to the experimental value for the Y-1:2:3 film, $\Phi(T_g)=0.82(\pi/2)$. Though the measured and calculated curves are qualitatively similar, a quantitative agreement is lacking. This is in agreement with the results of Kirkpatrick[44] on random resistor networks, where numerical calculations and the effective medium approximation agree for $\Delta p \gtrsim 0.1$. However, the effective medium approximation shows that the phase angle Φ is frequency independent at the percolation transition for $\omega \ll \omega_0$. The critical loss tangent in the EMA is $\tan(\Phi_c)=1$ in contrast to the value $\tan(\Phi_c)=2.13\pm0.18$ found numerically[24] for $d=3$.

In $d=3$ dimensions the loss tangent shows an upturn at large frequencies $\omega/\omega_0 \gtrsim 1$; see Fig. 4(a). This is not in disagreement with the scaling law, Eq. (15), which is only valid at low frequencies. Since $\omega_0 \simeq 10^6 - 10^{12}$ Hz can be of the same order of magnitude as the depinning frequency $\tau_\eta^{-1} \simeq 10$ GHz, the approximate vortex glass conductivity $D_{VG}=i\omega\lambda_c^2$ should not be used at high frequencies

$\omega/\omega_0 \gtrsim 1$. In Figs. 5(a) and 5(b) the loss tangent and the conductivity modulus are shown in $d=3$ dimensions using the vortex glass diffusivity, Eq. (9), $D_{VG}=i\omega\lambda_c^2/(1+i\omega\tau_\eta)$ with $\tau_\eta^{-1}=100\omega_0$. The Magnus force term is neglected, $\beta=0$. At large frequencies $\omega \gg \tau_\eta^{-1}$ the loss tangent above and below the percolation transition decreases as $\tan(\Phi) \propto \omega^{-1}$. This asymptotic form is in agreement with recent experimental results on Y-1:2:3 films.[30]

III. SUMMARY AND CONCLUSIONS

In this work the vortex motion in high-temperature superconductors was analyzed in a bond percolation model on a lattice. The linear, frequency-dependent electronic conductivity $\sigma(\omega)$ is found to be inversely proportional to the vortex diffusivity. Near the percolation threshold p_c the electronic conductivity obeys scaling laws that assume the same limiting forms as the scaling laws derived in vortex glass theory. Therefore the percolation model provides an alternative interpretation for the existence of a scaling region in $\sigma(\omega)$. The vortex glass transition temperature T_g is equivalent to the percolation threshold p_c.

The ratio of the critical exponents, $t/s=2.0\pm0.4$, observed experimentally in YBa$_2$Cu$_3$O$_{7-\delta}$ single crystals[8,9] and ceramics[38] is consistent with the critical exponents for bond percolation on a 3D lattice,[24] $t/s=2.60\pm0.14$. This is particularly surprising since the percolating vortices in superconductors are line objects, whereas point particles are assumed in the simulations of bond percolation models. How-
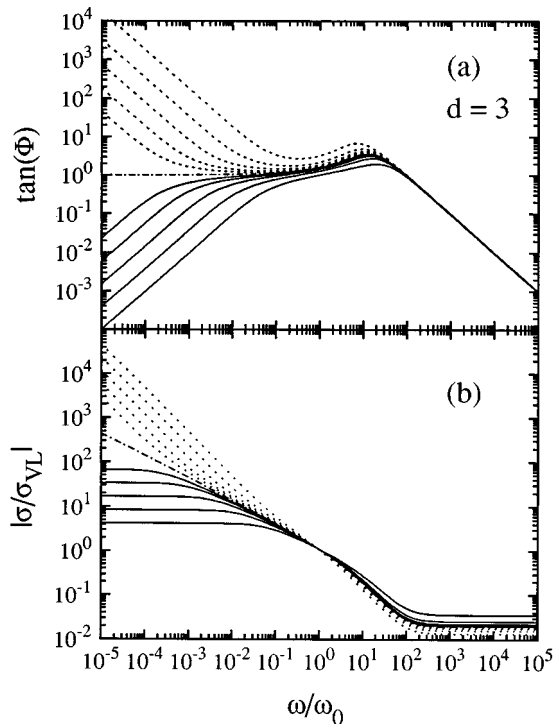
FIG. 5. (a) Loss tangent and (b) modulus of the electronic conductivity in the effective medium approximation for $d = 3$ dimensions. The parameters are $\tau_\beta = 0$ and $\omega_0 \tau_\eta = 0.01$. The dash-dotted line is the percolation transition $p = p_c$, and the dotted and solid lines are calculated in the vortex glass and vortex liquid phase for concentrations $|\Delta p| = 0.01, 0.02, 0.04, 0.08, 0.16$.

ever, the longitudinal correlation length of vortices in high-temperature superconductors is quite small[47] and therefore the treatment of individual vortex segments as point particles

might be justified. The agreement between the calculated and measured ratio of the critical exponents t/s in Y-1:2:3 twinned single crystals[8,9] and ceramics[38] indicates the presence of two pinning mechanisms with significantly different activation energies. The different pinning mechanisms may be related to pinning by point defects and to pinning by extended defects.

The ratio of the critical exponents observed in YBa$_2$Cu$_3$O$_{7-\delta}$ films,[35,10,37] $t/s = 4.4 \pm 0.7$, is considerably higher than the theoretical value, indicating the presence of a continuous distribution of bond diffusivities.

Calculations of the electronic conductivity in an effective medium approximation show qualitative agreement with measured conductivities. Using a transfer matrix approach the scaling functions in the bond percolation model can be obtained numerically.[48]

The percolation model of vortex motion in inhomogeneous superconductors is valid if percolative channels for vortex motion are well defined. Well-defined channels might be expected, if the ''pinning time'' $\tau_p \propto \exp(U/kT)$, i.e., the average time the vortex lines stay at their pinning centers, is long compared to the probing time scale. Since all investigated Y-1:2:3 samples show a scaling region in the linear electronic conductivity around the vortex glass temperature T_g, one might conclude that a well-defined percolation network exists in these samples. However, for Bi$_2$Sr$_2$CaCu$_2$O$_8$ single crystals in a magnetic field $B = 1$ T parallel to the c axis the absence of critical scaling in the electronic conductivity is reported.[49] Since Bi-2:2:1:2 single crystals have much smaller activation energies U than Y-1:2:3 samples,[17] the ''pinning times'' τ_p are considerably smaller and an ill-defined percolation network might result.

[*]Present address: University of Leipzig, Department of Superconductivity and Magnetism, Linnéstraße 5, D-04103 Leipzig, Germany.

[1]M.P.A. Fisher, Phys. Rev. Lett. **62**, 1415 (1989); D.S. Fisher, M.P.A. Fisher, and D.A. Huse, Phys. Rev. B **43**, 130 (1991).

[2]A.T. Dorsey, M. Huang, and M.P.A. Fisher, Phys. Rev. B **45**, 523 (1992).

[3]C.J. van der Beek, V.B. Geshkenbein, and V.M. Vinokur, Phys. Rev. B **48**, 3393 (1993).

[4]A.E. Koshelev and V.M. Vinokur, Physica C **173**, 465 (1991).

[5]P.H. Kes, J. Aarts, J. van den Berg, C.J. van der Beek, and J.A. Mydosh, Supercond. Sci. Technol. **1**, 242 (1989).

[6]M.W. Coffey and J.R. Clem, Phys. Rev. Lett. **67**, 386 (1991).

[7]E.H. Brandt, Phys. Rev. Lett. **67**, 2219 (1991).

[8]D.S. Reed, N.-C. Yeh, W. Yiang, U. Kriplani, D.A. Beam, and F. Holtzberg, Phys. Rev. B **49**, 4384 (1994).

[9]J. Kötzler, M. Kaufmann, G. Nakielski, R. Behr, and W. Assmus, Phys. Rev. Lett. **72**, 2081 (1994).

[10]J. Kötzler, G. Nakielski, M. Baumann, R. Behr, F. Goerke, and E.H. Brandt, Phys. Rev. B **50**, 3384 (1994).

[11]R.H. Koch, V. Foglietti, W.J. Gallagher, G. Koren, A. Gupta, and M.P.A. Fisher, Phys. Rev. Lett. **63**, 1511 (1989).

[12]P.L. Gammel, L.F. Schneemeyer, and D.J. Bishop, Phys. Rev. Lett. **66**, 953 (1991).

[13]H.S. Bokil and A.P. Young, Phys. Rev. Lett. **74**, 3021 (1995).

[14]D. Dew-Hughes, Cryogenics **28**, 674 (1988).

[15]V.B. Geshkenbein, V.M. Vinokur, and R. Fehrenbacher, Phys. Rev. B **43**, 3748 (1991).

[16]M. Golosovsky, M. Tsindlekht, H. Chayet, and D. Davidov, Phys. Rev. B **50**, 470 (1994).

[17]C.J. van der Beek and P.H. Kes, Phys. Rev. B **43**, 13 032 (1991).

[18]M. Ziese, P. Esquinazi, and H.F. Braun, Supercond. Sci. Technol. **7**, 869 (1994).

[19]S. Fleshler, W.K. Kwok, U. Welp, V.M. Vinokur, M.K. Smith, J. Downey, and G.W. Crabtree, Phys. Rev. B **47**, 14 448 (1993).

[20]C. Tomé-Rosa, G. Jakob, A. Walkenhorst, M. Maul, M. Schmitt, M. Paulson, and H. Adrian, Z. Phys. B **83**, 221 (1991).

[21]E.J. Tomlinson, P. Przyslupski, and J.E. Evetts, Cryogenics **33**, 28 (1993); R.A. Doyle, D. Kumar, P. Pullan, R. Gross, A.M. Campbell, M.G. Blamire, R.E. Somekh, and J.E. Evetts, in *Applied Superconductivity*, Proceedings of EUCAS '93, edited by H.C. Freyhardt (DGM Informationsgesellschaft, Oberursel, 1993), p. 689.

[22]A. Gurevich, Phys. Rev. B **42**, 4857 (1990); A. Gurevich, H. Küpfer, and C. Keller, Europhys. Lett. **15**, 789 (1991).

[23]R. Wördenweber, Phys. Rev. B **46**, 3076 (1992).

[24]J.P. Clerc, G. Giraud, J.M. Laugier, and J.M. Luck, Adv. Phys. **39**, 191 (1990).

[25] E.H. Brandt, Z. Phys. B **80**, 167 (1990).

[26] V.M. Vinokur, V.B. Geshkenbein, M.V. Feigel'man, and G. Blatter, Phys. Rev. Lett. **71**, 1242 (1993).

[27] R. Labusch, Cryst. Lattice Defects **1**, 1 (1969).

[28] A.M. Campbell, J. Phys. C **2**, 1492 (1969); **4**, 3186 (1971).

[29] D.H. Wu and S. Sridhar, Phys. Rev. Lett. **65**, 2074 (1990).

[30] D.H. Wu, J.C. Booth, and S.M. Anlage, Phys. Rev. Lett. **75**, 525 (1995).

[31] Straley and Kenkel investigated random resistor networks with nonlinear I-V characteristics [J.P. Straley and S.W. Kenkel, Phys. Rev. B **29**, 6299 (1984)]. They showed that far from the percolation threshold the averaged I-V characteristic is similar to the I-V characteristic of the individual network element, whereas a power law behavior prevails close to p_c. For the special case of power law I-V characteristics $V = r|I|^a \mathrm{sgn}I$ they found the critical exponent t in two dimensions to be only weakly dependent on the exponent a. Roux and Herrmann investigated two-dimensional resistor networks with individual circuit elements that had random voltage thresholds and obtained a power law behavior of the averaged I-V characteristic at the percolation threshold [S. Roux and H.J. Herrmann, Europhys. Lett. **4**, 1227 (1987)]. The existence of a universal power law in the I-V characteristics at T_g is commonly regarded as a signature of the vortex glass transition.

[32] K. Yamafuji and T. Kiss, Physica C **258**, 197 (1996).

[33] D.S. Reed, N.-C. Yeh, W. Jiang, U. Kriplani, and F. Holtzberg, Phys. Rev. B **47**, 6150 (1993).

[34] Y. Ando, H. Kubota, Y. Sato, and I. Terasaki, Phys. Rev. B **50**, 9680 (1994).

[35] H.K. Olsson, R.H. Koch, W. Eidelloth, and R.P. Robertazzi, Phys. Rev. Lett. **66**, 2661 (1991).

[36] H. Wu, N.P. Ong, and Y.Q. Li, Phys. Rev. Lett. **71**, 2642 (1993).

[37] L. Baselgia Stahel, B. Schmied, M. Calame, Ch. Leemann, Ph. Luginbuhl, and P. Martinoli, Physica C **235−240**, 2665 (1994).

[38] G. Nakielski, M. Kaufmann, S. Gauss, and J. Kötzler, Physica C **235−240**, 2667 (1994).

[39] J.M. Normand (unpublished).

[40] J.M. Normand and H.J. Herrmann, Int. J. Mod. Phys. C **1**, 207 (1990).

[41] B. Derrida, D. Stauffer, H.J. Herrmann, and J. Vannimenus, J. Phys. (Paris) Lett. **44**, L701 (1983).

[42] S. Feng, B.I. Halperin, and P.N. Sen, Phys. Rev. B **35**, 197 (1987).

[43] T.C. Lubensky and A.-M.S. Tremblay, Phys. Rev. B **34**, 3408 (1986).

[44] S. Kirkpatrick, Rev. Mod. Phys. **45**, 574 (1973).

[45] D.A.G. Bruggemann, Ann. Phys. (Leipzig) **24**, 636 (1935).

[46] R. Landauer, J. Appl. Phys. **23**, 779 (1952).

[47] O. Brunner, L. Antognazza, J.-M. Triscone, L. Miéville, and Ø. Fischer, Phys. Rev. Lett. **67**, 1354 (1991).

[48] J.M. Laugier, J.P. Clerc, G. Giraud, and J.M. Luck, J. Phys. A **19**, 3153 (1986); J.M. Laugier and J.M. Luck, J. Phys. A **20**, L885 (1987).

[49] R. Behr, J. Kötzler, G. Nakielski, M. Baumann, M. Kaufmann, and J. Kowalewski, Physica C **235−240**, 2669 (1994).